Reduced function of the glutathione S-transferase S1 suppresses behavioral hyperexcitability in *Drosophila* expressing a mutant voltage-gated sodium channel

Hung-Lin Chen*,[1], Junko Kasuya†, Patrick Lansdon*,[2], Garrett Kaas*,[3], Hanxi Tang‡, Maggie Sodders†, and Toshihiro Kitamoto*,†

*Interdisciplinary Graduate Program in Genetics, †Department of Anesthesia, Carver College of Medicine, ‡Iowa Center for Research by Undergraduates, University of Iowa, IA 52242

[1]Current affiliation: Department of Medical Research, Tungs' Taichung MetroHarbor Hospital, Taichung City, Taiwan 43503, ROC

[2]Current affiliation: Department of Molecular Biosciences, College of Liberal Arts and Sciences, University of Kansas, KS 66045, USA

[3]Current affiliation: Department of Pharmacology, Vanderbilt University School of Medicine, Nashville, TN 37232, USA

Running title

Genetic suppression of fly seizures

Key words

Forward genetic screen, genetic modifiers, epilepsy, RNA-sequencing analysis

Corresponding author

Toshihiro Kitamoto, Ph.D.

Department of Anesthesia, Carver College of Medicine, University of Iowa, 1-316 BSB, 51 Newton Road, Iowa City, IA 52242

Tel 319-335-7924, Fax 319-356-2940, E-mail toshi-kitamoto@uiowa.edu

Acknowledgements

We thank Mr. Ryan Jewell and Mr. Pei-Jen Wang (Department of Medical Research, Tungs' Taichung MetroHarbor Hospital, Taichung City, Taiwan 43503, ROC) for their technical assistance.

ABSTRACT

Voltage-gated sodium (Na_v) channels play a central role in the generation and propagation of action potentials in excitable cells such as neurons and muscles. To determine how the phenotypes of Na_v-channel mutants are affected by other genes, we performed a forward genetic screen for dominant modifiers of the seizure-prone, gain-of-function *Drosophila melanogaster* Na_v-channel mutant, $para^{Shu}$. Our analyses using chromosome deficiencies, gene-specific RNA interference, and single-gene mutants revealed that a null allele of *glutathione S-transferase S1* (*GstS1*) dominantly suppresses $para^{Shu}$ phenotypes. Reduced *GstS1* function also suppressed phenotypes of other seizure-prone Na_v-channel mutants, $para^{GEFS+}$ and $para^{bss}$. Notably, $para^{Shu}$ mutants expressed 50% less *GstS1* than wild-type flies, further supporting the notion that $para^{Shu}$ and *GstS1* interact functionally. Introduction of a loss-of-function *GstS1* mutation into a $para^{Shu}$ background led to up- and down-regulation of various genes, with those encoding cytochrome P450 (CYP) enzymes most significantly over-represented in this group. Because *GstS1* is a fly ortholog of mammalian hematopoietic prostaglandin D synthase, and in mammals CYPs are involved in the oxygenation of polyunsaturated fatty acids including prostaglandins, our results raise the intriguing possibility that bioactive lipids play a role in *GstS1*-mediated suppression of $para^{Shu}$ phenotypes.

INTRODUCTION

Defects in ion-channel genes lead to a variety of human disorders that are collectively referred to as channelopathies. These include cardiac arrhythmias, myotonias, forms of diabetes and an array of neurological diseases such as epilepsy, familial hyperekplexia, and chronic pain syndromes (RAJAKULENDRAN *et al.* 2012; VENETUCCI *et al.* 2012; WAXMAN AND ZAMPONI 2014; DIB-HAJJ *et al.* 2015; JEN *et al.* 2016). The advent of genome-wide association studies and next-generation sequencing technology has made the identification of channelopathy mutations easier than ever before. However, the expressivity and disease severity are profoundly affected by interactions between the disease-causing genes and gene variants at other genetic loci. The significance of gene-gene interactions in channelopathies was demonstrated by Klassen et al. (2011), who performed extensive parallel exome sequencing of 237 human ion-channel genes and compared variation in the profiles between patients with the sporadic idiopathic epilepsy and unaffected individuals. The combined sequence data revealed that rare missense variants of known channelopathy genes were prevalent in both unaffected and disease groups at similar complexity. Thus, the effects of even deleterious ion-channel mutations could be compensated for by variant forms of other genes (KLASSEN *et al.* 2011).

Drosophila offers many advantages as an experimental system to elucidate the mechanisms by which genetic modifiers influence the severity of channelopathies because of the: wealth of available genomic information, advanced state of the available genetic tools, short life cycle, high fecundity, and evolutionary conservation of biological pathways (HALES *et al.* 2015; UGUR *et al.* 2016). In the current study, we focused on genes that modify phenotypes of a voltage-gated sodium (Na_V)-channel mutant in *Drosophila*. Na_V-channels play a central role in the generation and propagation of action potentials in excitable cells such as neurons

and muscles (HODGKIN AND HUXLEY 1952; CATTERALL 2012). In mammals, the Na_v-channel gene family comprises nine paralogs. These genes encode large (~260 kDa) pore-forming Na_v-channel α-subunits, $Na_v1.1$- $Na_v1.9$, all of which have distinct channel properties and unique patterns of expression involving both subsets of neurons and other cell types. The *Drosophila* genome contains a single Na_v-channel gene, *paralytic* (*para*), on the X chromosome. It encodes Na_v-channel protein isoforms that share high amino-acid sequence identity/similarity with mammalian counterparts (e.g., 45%/62% with the human Na_v 1.1). High functional diversity of *para* Na_v channels is achieved through extensive alternative splicing that produces a large number (~60) of unique transcripts (KROLL *et al.* 2015).

A number of *para* mutant alleles have been identified in *Drosophila*. They display a variety of physiological and behavioral phenotypes: lethality, olfactory defects, spontaneous tremors, neuronal hyperexcitability, resistance to insecticides, and paralysis or seizure in response to heat, cold, or mechanical shock (SUZUKI *et al.* 1971; GANETZKY AND WU 1982; LILLY *et al.* 1994; MARTIN *et al.* 2000; LINDSAY *et al.* 2008; PARKER *et al.* 2011; SUN *et al.* 2012; SCHUTTE *et al.* 2014; KAAS *et al.* 2016). One of these more recently characterized Na_v-channel gene mutants, $para^{Shu}$, is a dominant gain-of-function allele formerly referred to as *Shudderer* due to the “shuddering” or spontaneous tremors it causes (WILLIAMSON 1971; WILLIAMSON 1982). This allele contains a missense mutation that results in the replacement of an evolutionarily conserved methionine residue in Na_v-channel homology domain III (Kaas et al. 2016). Adult $para^{Shu}$ mutants exhibit various dominant phenotypes in addition to shuddering, such as defective climbing behavior, increased susceptibility to electroconvulsive and heat-induced seizures, and short lifespan. They also have an abnormal down-turned wing posture and an indented thorax, both of which are thought to be caused by neuronal hyperexcitability (WILLIAMSON 1982; KAAS *et al.* 2016; KASUYA *et al.* 2019). In the current study, we carried out a

forward genetic screen for dominant modifiers of *para*^{Shu} and found that the phenotypes are significantly suppressed by loss-of-function mutations in the *glutathione S-transferase S1* (*GstS1*) gene. To obtain insights into the mechanisms underlying this GstS1-mediated suppression of *para*^{Shu} phenotypes, we also performed RNA-sequencing analysis. This revealed changes in gene expression that are caused by reduced *GstS1* function in the *para*^{Shu} background.

MATERIALS AND METHODS

Fly stocks and culture conditions

Flies were reared at 25°C, 65% humidity in a 12 hr light/dark cycle on a cornmeal/glucose/yeast/agar medium supplemented with the mold inhibitor methyl 4-hydroxybenzoate (0.05 %). The exact composition of the fly food used in this study was described in Kasuya et al. (2019). The *Canton-S* (*CS*) strain was used as the wild-type control. *para*^{Shu}, which was originally referred to as *Shudderer* (*Shu*) (WILLIAMSON 1982) and was obtained from Mr. Rodney Williamson (Beckman Research Institute of the Hope, CA). *Drosophila* lines carrying deficiencies of interest and a UAS-*GstS1* RNAi (GD16335) were obtained from the Bloomington Stock Center (Indiana University, IN) and the Vienna *Drosophila* Resource Center (Vienna, Austria), respectively. *GstS1*^{M26} was obtained from Dr. Tina Tootle (University of Iowa, IA). Genetic epilepsy with febrile seizures plus (GEFS+) and Dravet syndrome (DS) flies (*para*$^{GEFS+}$ and *para*^{DS}) (SUN *et al.* 2012; SCHUTTE *et al.* 2014) were obtained from Dr. Diane O'Dowd (University of California, Irvine, CA), and *bangsenseless* (*para*^{bss1}) flies were obtained from Dr. Chun-Fang Wu (University of Iowa, IA).

Behavioral assays

Reactive climbing: The reactive climbing assay was performed as previously described (KAAS *et al.* 2016), using a countercurrent apparatus originally invented by Seymour Benzer (BENZER 1967). Five to seven-day-old females (~20) were placed into one tube (tube #0), tapped to the bottom, and allowed 15 sec to climb, at which point those that had climbed were transferred to the next tube. This process was repeated a total of 5 times. After the fifth trial, the flies in each tube (#0 ~ #5) were counted. The climbing index (CI) was calculated using the following formula: $CI = \Sigma(Ni \times i)/(5 \times \Sigma Ni)$, where i and Ni represent the tube number (0-5) and the number of flies in the corresponding tube, respectively. For each genotype, at least 3 groups were tested.

Video-tracking locomotion analysis: Five-day-old flies were individually transferred into a plastic well (15 mm diameter x 3 mm depth) and their locomotion was recorded at 30 frames per second (fps) using a web camera at a resolution of 320 x 240 pixels for 10 minutes. The last 5 minutes of the movies were analyzed using pySolo, a multi-platform software for the analysis of sleep and locomotion in *Drosophila,* to compute the x and y coordinates of individual flies during every frame (GILESTRO AND CIRELLI 2009). When wild-type flies are placed in a circular chamber, they spend most of their time walking along the periphery (Besson and Martin 2005), resulting in circular tracking patterns. In contrast, the uncoordinated movements caused by spontaneous tremor or jerking of $para^{Shu}$ mutants lead to their increased presence in the center part of the chambers. The tremor frequency was therefore indirectly assessed by determining the percentage of time that fly stayed inside a circle whose radius is 74.3% of that of the entire chamber. The distance between the fly's position and the center of the chamber was calculated using the formula $(X_i-X_c)^2+(Y_i-Y_c)^2<13^2$ where X_i and Y_i

are the coordinates of the fly, and X_c and Y_c are the coordinates of the chamber center (13 mm is 74.3 % of the chamber radius).

Heat-induced seizures: Newly eclosed flies were collected in groups of 20 and aged for 3 to 5 days, after which the heat-induced seizure assay was performed as previously described (SUN *et al.* 2012). Briefly, a single fly was put into a 15 x 45 mm glass vial at room temperature (Thermo Fisher Scientific, MA) and allowed to acclimate for 2 to 10 minutes. The glass vial was then submerged in a water bath at the specified temperature for 2 minutes, during which the fly was video-taped and assessed for seizure behavior every 5 seconds. Seizure behavior was defined as loss of standing posture followed by leg shaking.

Bang-sensitive assay: The bang-sensitive assay was carried out following a previously described protocol (ZHANG *et al.* 2002). Briefly, 10 flies were raised on conventional food for 2-3 days post-eclosion. Prior to testing, individual flies were transferred to a clean vial and acclimated for 30 minutes. Next, the vials were vortexed at maximum speed for 10 seconds, and the time to recovery was measured. Recovery was defined as the ability of flies to stand upright following paralysis. At least 5 independent bang-sensitive assays were carried out for each genotype.

Male mating assay: Newly eclosed $para^{Shu}$ males with or without one or two copies of $GstS1^{M26}$ (i.e., $para^{Shu}$/Y ; +/+, $para^{Shu}$/Y ; $GstS1^{M26}$/+, and $para^{Shu}$/Y ; $GstS1^{M26}$/$GstS1^{M26}$) were collected. Each was placed, along with 3-5 day-old wild-type (*Canton-S*) virgin females, into a plastic tube (75 x 12 mm) containing approximately 1 ml of fly food. Tubes were kept at room temperature (~ 22ºC) for two weeks, at which point they were examined for the presence of progeny.

Gene expression analysis

RNA was purified from one-day-old female flies using Trizol solution (Ambion, Carlsbad, CA) and an RNasy column (Qiagen, Valencia, CA). Flies of four genotypes were used: (1) +/+ ; +/+, (2) $para^{Shu}$/+ ; +/+, (3) +/+ ; $GstS1^{M26}$/+, and (4) $para^{Shu}$/+ ; $GstS1^{M26}$/+. For each genotype, RNA-sequence (RNA-seq) analysis was performed (four biological replicates) by the Iowa Institute of Human Genetics (IIHG) Genomics Division (University of Iowa, Iowa). DNase I-treated total RNA (500 ng) samples were enriched for PolyA-containing transcripts by treatment with oligo(dT) primer-coated beads. The enriched RNA pool was then fragmented, converted to cDNA, and ligated to index-containing sequence adaptors using the Illumina TruSeq Stranded mRNA Sample Preparation Kit (Cat. #RS-122-2101, Illumina, Inc., San Diego, CA). The molar concentrations of the indexed libraries were measured using the 2100 Agilent Bioanalyzer (Agilent Technologies, Santa Clara, CA) and combined equally into pools for sequencing. The concentrations of the pools were measured using the Illumina Library Quantification Kit (KAPA Biosystems, Wilmington, MA) and the samples were sequenced on the Illumina HiSeq 4000 genome sequencer using 150 bp paired-end SBS chemistry.

Sequences in FASTQ format were analyzed using the Galaxy platform (https://usegalaxy.org/). The FASTQ files were first evaluated using a quality-control tool, FastQC. The sequenced reads were filtered for those that met two conditions: minimum length >20 and quality cutoff >20. After the quality control assessments were made, the reads were mapped to Release 6 of the *Drosophila melanogaster* reference genome assembly (dm6) using the STAR tool. The number of reads per annotated gene was determined by running the featureCounts tool. The differential gene expression analyses were performed using the DESeq2 tool (LOVE *et al.* 2014), which uses the median of ratios method to normalize counts. The *P*-value was adjusted (P_{adj}) for multiple testing using the Benjamini-Hochberg procedure,

which controls for the false discovery rate (FDR). For functional enrichment analysis of differentially expressed genes (DEGs), we generated a list of those for which P_{adj}<0.05 and applied it to the GOseq tool for gene ontology analysis (YOUNG *et al.* 2010).

Statistical analysis

Statistical tests were performed using Sigma Plot (Systat Software, San Jose, CA). For multiple groups that exhibit non-normal distributions, the Kruskal-Wallis one-way ANOVA on ranks test was performed using Dunn's method *post hoc*. Data that did not conform to a normal distribution are presented as box-and-whisker plots (boxplots). Values of the first, second, and third quartiles (box) are shown, as are the 10th and 90th percentiles (whisker), unless otherwise stated. Two-way repeated measures ANOVA and Holm-Sidak multiple comparisons were used to analyze temperature-induced behavioral phenotypes. Fisher's exact test was used to analyze the wing and thorax phenotypes of *para*^{Shu} mutants. For multiple comparison, the *P*-values were compared to the Bonferroni adjusted type I error rate for significance. Statistical analyses for RNAseq experiments are described in the previous section "Gene expression analysis by RNA-sequencing".

RESULTS

The chromosomal region 53F4-53F8 contains a dominant modifier(s) of *para*^{Shu}

To identify genes that interact with *para*^{Shu} and influence the severity of the phenotype, we performed a forward genetic screen for dominant modifiers of *para*^{Shu} using the Bloomington Deficiency Kit (COOK *et al.* 2012; ROOTE AND RUSSELL 2012). Females

heterozygous for *para*^{Shu} (*para*^{Shu}/*FM7*) were crossed to males carrying a deficiency on the second or third chromosome (+/Y ; *Df(2)*/balancer or +/Y ;; *Df(3)*/balancer). The effects of the deficiency on *para*^{Shu} were evaluated by examining the F1 female progeny trans-heterozygous for *para*^{Shu} and the deficiency (e.g., *para*^{Shu}/+ ; *Df*/+) for their reactive climbing behavior (see Materials and Methods). As reported previously, *para*^{Shu} heterozygous females have a severe defect in climbing behavior due to spontaneous tremors and uncoordinated movements (KAAS *et al.* 2016). Our initial screen identified several chromosomal deficiencies that significantly improved the climbing behavior of *para*^{Shu} females (Supplemental Table 1; deficiencies that resulted in CI>0.4 are shaded). The current study focuses on one of these deficiencies, *Df(2R)P803-Δ15*.

The *Df(2R)P803-Δ15* deficiency spans chromosomal region 53E-53F11 on the right arm of the second chromosome, but a lack of nucleotide level information regarding its break points made identifying the genomic region responsible for suppression of the *para*^{Shu} phenotypes challenging. Therefore, we used three additional deficiencies which overlap *Df(2R)P803-Δ15* and also have molecularly defined break points (Figure 1A). Phenotypic analysis of *para*^{Shu} females crossed to these deficiencies revealed that *Df(2R)Exel6065* and *Df(2R)BSC433*, but not *Df(2R)Exel6066*, had a robust suppressing effect similar to that of *Df(2R)P803-Δ15* (Figure 1B). Of the two suppressing alleles, *Df(2R)BSC433* carries the smaller deficiency; it spans genomic region 53F4 to 53F8 (Figure 1A).

The suppressive effect of *Df(2R)BSC433* was confirmed by analyzing other *para*^{Shu} phenotypes. The introduction of *Df(2R)BSC433* to the *para*^{Shu} background (*para*^{Shu}/+ ; *Df(2R)BSC433*/+) significantly reduced the severity of the abnormal wing posture, indented thorax (Figure 2A), spontaneous tremors (Figure 2B), and heat-induced seizures (Figure 2C). Two deficiency lines, *Df(2R)BSC273* (49F4-50A13) and *Df(2R)BSC330* (51D3-51F9), carry a

genetic background comparable to that of *Df(2R)BSC433*. Unlike *Df(2R)BSC433*, these deficiencies did not lead to suppression of *para^{Shu}* phenotypes (Figure 2A-C), showing that the effect of *Df(2R)BSC433* is not due to its genetic background. Taken together, these results clearly demonstrate that removal of one copy of the genomic region 53F4-53F8 reduces the severity of multiple *para^{Shu}* phenotypes, and that a dominant *para^{Shu}* modifier is present in this chromosomal segment.

***GstS1* loss of function suppresses *para^{Shu}* phenotypes**

Based on the molecularly defined breakpoints of *Df(2R)BSC433* (2R:17,062,915 and 2R:17,097,315), it disrupts six genes that are localized in the 53F4-53F8 region: *CG8950*, *CG6967*, *CG30460*, *CG8946* (*Sphingosine-1-phosphate lyase*; *Sply*), *CG6984*, and *CG8938* (*Glutathione S-transferase S1*; *GstS1*) (Figure 3A). To identify the gene(s) whose functional loss contributes to the marked suppression of *para^{Shu}* phenotypes by *Df(2R)BSC433*, we knocked down each gene separately using gene-specific RNAi and examined the effects on *para^{Shu}* phenotypes. Expression of each RNAi transgene of interest was driven by the ubiquitous Gal4 driver, *da-Gal4*. RNAi-mediated knockdown of *CG6967* or *Sply* resulted in developmental lethality, whereas knockdown of *CG8950*, *CG30460*, *CG6984* or *GstS1* did not. Among the viable adult progeny with gene-specific knockdown, those in which *Gst1S1* was knocked down showed the greatest improvement in wing and thorax phenotypes (Figure 3B). Thus, reduced *GstS1* function likely contributes to the suppression of *para^{Shu}* phenotypes by *Df(2R)BSC433*.

GstS1^{M26} is a null allele of *GstS1* in which the entire coding region is deleted (WHITWORTH *et al.* 2005) and homozygotes are viable as adults. We used *GstS1^{M26}* to determine how reduced *GstS1* function affects *para^{Shu}* phenotypes. In *para^{Shu}*/+ ; *GstS1^{M26}*/+

flies, both the morphological (downturned wing and indented thorax) and behavioral (spontaneous tremors and heat-induced seizure) phenotypes were considerably milder than in their *para*^{Shu}/+ counterparts (Figure 4A-C). *para*^{Shu} phenotypes were not further improved in *GstS1*^{M26} homozygotes (*para*^{Shu}/+ ; *GstS1*^{M26}/*GstS1*^{M26}), where *GstS1* function was completely eliminated (Figure 4A-C). Thus, *GstS1*^{M26} is a dominant suppressor of female *para*^{Shu} phenotypes.

GstS1^{M26} reduced the severity of the male *para*^{Shu} phenotypes as well, including not only viability, but also courtship behavior and copulation. With respect to viability, *para*^{Shu} males represented only 8.2% of the male progeny (*para*^{Shu}/Y and *FM7*/Y) of a cross between *para*^{Shu}/*FM7* females and wild-type males. Viability was significantly higher when one or two copies of *GstS1*^{M26} were introduced into *para*^{Shu} males (*para*^{Shu}/Y ; *GstS1*^{M26}/+ and *para*^{Shu}/Y ; *GstS1*^{M26}/*GstS1*^{M26}), with *para*^{Shu} males carrying *GstS1*^{M26} representing 31.4% and 53.1% of the total male progeny, respectively (Table 1). The effects of *para*^{Shu} on male courtship behavior/copulation are a consequence of the strong morphological (down-turned wings and indented thorax) and behavioral (spontaneous tremors and uncoordinated movements) phenotypes. When *para*^{Shu} males were individually placed into small tubes with four wild-type virgin females and food, only one out of 43 (2.3%) produced progeny. The introduction of *GstS1*^{M26} improved the ability to produce progeny; 17 out of 45 *para*^{Shu} males (37.8%) heterozygous for *GstS1*^{M26}, and 17 out of 44 *para*^{Shu} males (38.6%) heterozygous for *GstS1*^{M26}, produced progeny under the above-mentioned conditions (Table 1).

Loss of function of other glutathione S-transferase genes does not suppress *para^{Shu}* phenotypes as that of *GstS1*

The *Drosophila melanogaster* genome contains 36 genes that encode cytosolic glutathione S-transferases (GSTs). These are classified as Delta (D), Epsilon (E), Omega (O), Theta (T), Zeta (Z), or Sigma (S) based on similarities in the amino-acid sequences of the encoded proteins (TU AND AKGUL 2005; SAISAWANG *et al.* 2012). *GstS1* is the sole *Drosophila* member of the S class GST genes. To determine whether reductions in the copy number of other GST genes have significant impacts on *para^{Shu}* phenotypes, we generated *para^{Shu}* mutants carrying chromosome deficiencies that remove the D, E, O, T, or Z class of GST genes. Given that genes encoding GSTs of the same class tend to form gene clusters, a single chromosome deficiency often removes multiple GST genes of the same class. For example, *Df(3R)Exel6164* (87B5-87B10) removes eleven GST genes of the D class (*GstD1-D11*) (Table 2). For GST genes on the autosomes, *para^{Shu}* females (*para^{Shu}*/*FM7*) were crossed to males carrying a GST deficiency on the second or third chromosome. For the two GST genes on the X chromosome (*GstT3* and *GstT4*), females carrying the deficiency (*Df*/*FM7*) were crossed to *para^{Shu}* males (*para^{Shu}*/Y) because males carrying this (*Df*/Y) were not viable. The female progeny carrying both *para^{Shu}* and a deficiency of interest were examined for their wing posture and thorax morphology. As shown in Table 2, as well as in Figure 2, removing one copy of *GstS1* in the context of *Df(2R)BSC433* resulted in significant suppression of both the down-turned wing and the indented thorax phenotypes of *para^{Shu}*, but this ability was not shared by any of the 36 other cytosolic GST genes. In some cases, however, there was partial suppression of one or the other phenotype. For example, when one copy of *GstT4* was removed (using *Df(1)Exel6245*), the wing phenotype, but not the thorax phenotype, was suppressed. Similarly, the indented thorax phenotype, but not the down-turned wing

phenotype, was reduced when *GstD1-D11* was removed (using *Df(3R)Exel6164*) and when *GstT1-T2* was removed (using *Df(2R)BSC132*).

GstS1^{M26} **suppresses the phenotypes of other *para* gain-of-function mutants**

We next examined whether phenotypes of other Na_v-channel mutants are similarly affected by reduced *GstS1* function. Generalized epilepsy with febrile seizures plus (GEFS+) and Dravet syndrome (DS) are common childhood-onset genetic epileptic encephalopathies (CLAES *et al.* 2001; CATTERALL *et al.* 2010). Sun et al. (2012) and Schutte et al. (2014) created *Drosophila para* knock-in alleles, gain-of-function *para^{GEFS+}* and loss-of-function *para^{DS}*, by introducing a disease-causing human GEFS+ or DS mutation at the corresponding position of the fly Na_v-channel gene. At 40ºC, *para^{GEFS+}* homozygous females and hemizygous males exhibit a temperature-induced seizure-like behavior that is similar to, but milder than, that observed in *para^{Shu}* flies (SUN *et al.* 2012; KAAS *et al.* 2016; KASUYA *et al.* 2019). *para^{DS}* flies lose their posture shortly after being transferred to 37ºC (SCHUTTE *et al.* 2014). The temperature-induced phenotype of *para^{GEFS+}* was significantly suppressed when a single copy of *GstS1^{M26}* was introduced into *para^{GEFS+}* males (*para^{GEFS+}*/Y ; *GstS1^{M26}*/+) (Figure 5A). In contrast, the severity of the phenotype in *para^{DS}* males was unaffected by a copy of *GstS1^{M26}* (*para^{GEFS+}*/Y ; *GstS1^{M26}*/+) (Figure 5B).

We also examined *para^{bss1}*, which is a hyperexcitable, gain-of-function *para* mutant allele that displays semi-dominant, bang-sensitive paralysis (PARKER *et al.* 2011). The severity of the *para^{bss1}* bang-sensitivity was evaluated as the time for recovery from paralysis that had been induced by mechanical stimulation (10 seconds of vortexing). All *para^{bss1}* flies were paralyzed immediately after this mechanical stimulation. By three minutes after mechanical stimulation, 92% of the *para^{bss1}* males carrying *GstS1^{M26}* (*para^{bss1}*/Y ; *GstS1^{M26}*/+) had

recovered from paralysis and were able to right themselves, whereas only 12.6% of *para*^{bss1} males had recovered. The median recovery time for *para*^{bss1} males carrying *GstS1*^{M26} was 88 seconds and that for *para*^{bss1} males was 160 seconds (Figure 5C).

RNA sequencing analysis revealed changes in gene expression caused by *para*^{Shu} and *GstS1*^{M26} mutations.

To gain insights into the molecular basis of the *GstS1*-dependent suppression of *para*^{Shu} phenotypes, we performed RNA sequencing (RNA-seq) analysis and examined the transcriptome profiles of *para*^{Shu} and wild-type females with or without *GstS1*^{M26}. Whole-body transcriptomes of one-day-old females were compared among four genotypes: (1) +/+ ; +/+, (2) *para*^{Shu}/+ ; +/+, (3) +/+ ; *GstS1*^{M26}/+, and (4) *para*^{Shu}/+ ; *GstS1*^{M26}/+. Each sample generated at least 21 million sequencing reads, of which >99% met the criteria of having a quality score of >20 and a length of >20 bp. Moreover, duplicate reads encompassed ~70% of total reads, which was expected from the RNA-seq data (BANSAL 2017).

We found that 129 genes were differentially expressed (threshold: adjusted *P*-value (P_{adj})<0.05) between *para*^{Shu} and wild-type females. Among these, 89 and 40 genes were up- and down-regulated, respectively, in *para*^{Shu} vs. wild-type flies (Supplemental Table 2). Gene ontology analysis of the differentially expressed genes was performed using GOseq tools (YOUNG *et al.* 2010). Genes associated with four Gene Ontology categories were found to be overrepresented within the dataset (P_{adj} <0.05), each with a functional connection to the chitin-based cuticle: “structural constituent of chitin-based larval cuticle (GO:0008010)”, “structural constituent of chitin-based cuticle (GO:0005214)”, “structural constituent of cuticle (GO:0042302)”, and “chitin-based cuticle development (GO:0040003)” (Table 3A). Within

these GO categories, eight genes were differentially expressed between *para*^{Shu} and wild-type flies (Table 3B).

Among the genes that are differentially regulated (P_{adj}<0.05) between wild-type and *para*^{Shu} flies (Supplemental Table 2), 16 displayed a fold change of >2 and all are up-regulated in *para*^{Shu} flies (Table 4). They encode: a transferase (*CG32581*), two lysozymes (*LysC* and *LysD*), two endopeptidases (*Jon25Bi* and *CG32523*), one endonuclease (*CG3819*), two cytochrome P450 proteins (*Cyp4p1 and Cyp6w1*), three ABC transporters (*l(2)03659, CG7300 and CG1494*), three transcription factors (*lmd, CG18446 and Ada1-1*), and two cuticle proteins (*Cpr47Ef and Ccp84Ab*). Of note, *GstS1* was one of the 40 genes that are significantly down-regulated in *para*^{Shu} females; the average normalized sequence counts (DESeq2) were 50% reduced (15562.21 vs 7782.01, adjusted P_{adj}=0.00036) (Table 5, Figure 6). In general, we did not observe any significant differences in the expression of other GST genes between *para*^{Shu} and wild-type flies, with the only exceptions being *GstD2* and *GstO2* (Table 5), down-regulated and up-regulated, respectively.

We next examined how *GstS1*^{M26} affects gene expression profiles in *para*^{Shu} mutants. The fact that *GstS1*^{M26} is a deletion mutation that removes the entire coding region of *GstS1* (WHITWORTH *et al.* 2005) is consistent with our discovery that the levels of the *GstS1* transcript were 50% lower than those in wild-type flies when one copy of *GstS1*^{M26} was introduced (Figure 6). Since *para*^{Shu} and *GstS1*^{M26} each reduced *GstS1* expression by ~50%, the level of *GstS1* expression in *para*^{Shu}; *GstS1*^{M26} double heterozygotes (*para*^{Shu}/+ ; *GstS1*^{M26}/+) was approximately one quarter of that in wild-type flies (Figure 6).

Comparison of *para*^{Shu} flies to *para*^{Shu} and *GstS1*^{M26} double mutants (*para*^{Shu}/+ ; +/+ vs. *para*^{Shu}/+ ; *GstS1*^{M26}/+) revealed the differential expression of 220 genes (for P_{adj}<0.05;

Supplemental Table 2). Among these, 120 were up-regulated and 100 were downregulated in *para*^{Shu} plus *GstS1*^{M26} flies. Functional enrichment analysis of the differentially expressed genes revealed that genes associated with five specific molecular functions were over-represented. These include “heme binding” (GO:0020037), “tetrapyrrole binding” (GO:0046906), “iron ion binding” (GO:0005506), “oxidoreductase activity, acting on paired donors, with incorporation or reduction of molecular oxygen” (GO:0016705), and “cofactor binding” (GO:0048037) (Table 6A). Thirteen differentially regulated genes were associated with all five GO terms. These all encode heme-containing enzymes CYPs (Table 6B, marked with asterisks) that catalyze a diverse range of reactions and are critical for normal developmental processes and the detoxification of xenobiotic compounds (Hannemann et al. 2007; Isin and Guengerich 2007; Chung et al. 2009).

Among the 220 genes differentially regulated in *para*^{Shu} in the absence or presence of *GstS1*^{M26} (*para*^{Shu}/+ ; +/+ vs. *para*^{Shu}/+ ; *GstS1*^{M26}/+), 25 were up-regulated and 12 were down-regulated (cutoff: fold change >2; Table 7). The gene for which the fold-change was greatest in *para*^{Shu} plus *GstS1*^{M26} flies was a member of the cytochrome P450 family, *Cyp4p2*; it was down-regulated 6.4-fold in the presence of *GstS1*^{M26}, with P_{adj}=3.5 x 10^{-48}. Notably, three of the top 20 genes with the greatest fold expression changes were members of this family (*Cyp4p2*, *Cyp6a8*, *Cyp6a2*).

DISCUSSION

In the present study, we performed an unbiased forward genetic screen to identify genes that have a significant impact on the phenotypes associated with *para*^{Shu}, a gain-of-function variant of the *Drosophila* Na_v channel gene. Our key finding was that a 50% reduction

of GstS1 function resulted in strong suppression of *para*^{Shu} phenotypes. Glutathione S-transferases (GSTs) are phase II metabolic enzymes that are primarily involved in conjugation of the reduced form of glutathione to endogenous and xenobiotic electrophiles for detoxification (HAYES *et al.* 2005; ALLOCATI *et al.* 2018). Reduced GST function is generally considered damaging to organisms because it is expected to lead to an accumulation of harmful electrophilic compounds in the cell and thereby disturb critical cellular processes. In fact, a previous study showed that loss of *GstS1* function enhanced the loss of dopaminergic neurons in a *parkin* mutant, a *Drosophila* model of Parkinson's disease and conversely, overexpression of *GstS1* in the same dopaminergic neurons suppressed dopaminergic neurodegeneration in such mutants (WHITWORTH *et al.* 2005). Parkin has ubiquitin-protein ligase activity (IMAI *et al.* 2000; SHIMURA *et al.* 2000; ZHANG *et al.* 2000) and the accumulation of toxic Parkin substrates likely contributes to the degeneration of dopaminergic neurons in Parkinson's patients and animal models (WHITWORTH *et al.* 2005). These results are consistent with the idea that GstS1 plays a role in the detoxification of oxidatively damaged products to maintain healthy cellular environments. In this regard, it seems counterintuitive that loss of *GstS1* function reduces, rather than increases, the severity of *para*^{Shu} phenotypes.

GstS1 is unique among *Drosophila* GSTs in several respects. A previous study, based on multiple alignments of GST sequences, had revealed that GstS1 is the sole member of the *Drosophila* sigma class of GST (AGIANIAN *et al.* 2003). Unlike other GSTs, GstS1 has low catalytic activity for typical GST substrates, such as 1-chloro-2,4-dinitrobenzol (CDNB), 1,2-dichloro-4-nitrobenzene (DCNB), and ethacrynic acid (EA). Instead, it efficiently catalyzes the conjugation of glutathione to 4-hydroxynonenal (4-HNE), an unsaturated carbonyl compound derived via lipid peroxidation (SINGH *et al.* 2001; AGIANIAN *et al.* 2003). The crystal structure of GstS1 indicates that its active-site topography is suitable for the binding of amphipolar lipid

peroxidation products such as 4-HNE (AGIANIAN *et al.* 2003), consistent with the above-mentioned substrate specificity. 4-HNE is the most abundant 4-hydroxyalkenal formed in cells and contributes to the deleterious effects of oxidative stress. It has been implicated in the pathogenesis and progression of human diseases such as cancer, Alzheimer's disease, diabetes, and cardiovascular disease (SHOEB *et al.* 2014; CSALA *et al.* 2015). However, 4-HNE also functions as a signaling molecule and has concentration-dependent effects on various cellular processes including differentiation, growth and apoptosis (ZHANG AND FORMAN 2017). GstS1 plays a major role in controlling the intracellular 4-HNE concentration to balance its beneficial and damaging effects; one study estimated that it is responsible for ~70% of the total capacity to conjugate 4-HNE with glutathione in adult *Drosophila* (SINGH *et al.* 2001). It is thus possible that in *para*^{Shu} flies the reduction of GstS1 activity enhances the strength of 4-HNE-dependent signaling, leading to changes in neural development and/or function that compensate for the defect caused by the *para*^{Shu} mutation.

Notably, GSTs are not limited to conjugating glutathione to potentially harmful substrates for their clearance, and it is possible that another such function accounts for our observations. Specifically, some GSTs catalyze the synthesis of physiologically important compounds. With respect to its primary amino acid sequence, *Drosophila* GstS1 is more similar to the vertebrate hematopoietic prostaglandin D2 synthases (HPGDSs) than to other *Drosophila* GSTs (AGIANIAN *et al.* 2003). Indeed, the sequence identity/similarity between *Drosophila* GstS1 and human HPGDS are 37%/59%, respectively. The *Drosophila* Integrative Ortholog Prediction Tool (DIOPT; http://www.flyrnai.org/diopt) (HU *et al.* 2011), as well as a recent and extensive bioinformatics analysis (SCARPATI et al. 2019), classified GstS1 as a fly ortholog of HPGDS, a sigma-class member of the GST family that catalyzes the isomerization of prostaglandin H_2 (PGH_2) to prostaglandin D_2 (PGD_2). Mammalian HPGDS is a critical

regulator of inflammation and the innate immune response (RAJAKARIAR *et al.* 2007; JOO AND SADIKOT 2012). In light of this observation, findings implicating GstS1 in the development and function of the innate immune system in insects are of interest. For example, in a lepidopteran *Spodoptera exigua*, the ortholog of *Drosophila* GstS1, SePGDS, was identified as PGD_2 synthase, with the addition of PGD_2, but not its precursor (arachidonic acid), rescuing immunosuppression in larvae in response to SePGDS knockdown (SAJJADIAN *et al.* 2019). Consistent with this finding, previous studies in *Drosophila* had revealed that overexpression of *GstS1* in hemocytes (the insect blood cells responsible for cellular immunity) leads to increases in the number of larval hemocytes (STOFANKO *et al.* 2008) and that GstS1 in hemocytes is increased ~10-fold at the onset of metamorphosis (REGAN *et al.* 2013). These results strongly support a significant role for GstS1 in the insect innate immune system. In addition, we previously found that genes involved in innate immune responses were up-regulated in the adult head of $para^{Shu}$ mutants (KAAS *et al.* 2016), suggesting that the neuronal hyperexcitability induced by gain-of-function $para^{Shu}$ Na_v channels might lead to activation of the innate immune system. In light of these observations and our current findings it is possibile that the reason that loss of GstS1 function reduces the severity of $para^{Shu}$ phenotypes is that it suppresses the innate immune response through hemocytes and prostaglandin-like bioactive lipids.

Another connection to the innate immune system is the discovery, based on our transcriptome analysis, that CYP genes are over-represented among the genes that are differentially expressed in the $para^{Shu}$ with a *GstS1* mutation (Table 5). CYP enzymes are involved in the oxygenation of a wide range of compounds, including eicosanoids such as prostaglandins. In mammals, activation of the innate immune response alters CYP expression and eicosanoid metabolism in an isoform-, tissue-, and time-dependent manner (THEKEN *et al.*

2011). *GstS1* loss of function may affect *para*^{Shu} phenotypes by changing the activities of CYP enzymes. Further studies are required to elucidate whether and how CYP genes, as well as the genes involved in innate immune response and bioactive lipid signaling, contribute to *GstS1*-mediated modulation of *para*^{Shu} phenotypes.

To obtain insight into functional significance of changes in gene expression, we classified differentially expressed genes. For the 89 genes that were up-regulated by *para*^{Shu} (*para*^{Shu}/+ vs. +/+), it is notable that 13 were down-regulated when *GstS1*^{M26} was also introduced (*para*^{Shu}/+ vs. *para*^{Shu}/+ ; *GstS1*^{M26}/+) and that all of the GO categories associated (P_{adj}<0.05) with this group of genes were related to the chitin-based cuticle (Table 3A). On the other hand, among the 40 genes down-regulated by *para*^{Shu}, only 2 (*CG5966* and *CG5770*) were up-regulated by *GstS1*^{M26}. Although *CG5770* is an uncharacterized gene, *CG5966* encodes proteins that are highly expressed in the larval and adult fat bodies and predicted to be involved in lipid catabolism. A human *CG5966* homolog encodes pancreatic lipase, which hydrolyzes triglycerides in the small intestine and is essential for the efficient digestion of dietary fat (DAVIS *et al.* 1991). Notably, changes in the expression of these cuticle-associated and fat metabolism-associated sets of genes appear to correlate with the phenotypic severity of *para*^{Shu} in that a change in the phenotype or gene expression induced by *para*^{Shu} is reversed by *GstS1*^{M26}. It is possible that changes in the expression of these genes is causative and contributes to the severity of *para*^{Shu} phenotypes. Alternatively, these changes in gene expression could be a consequence of phenotypic changes caused by other factors. Further functional analysis is required to determine the significance of these genes in controlling *para*^{Shu} phenotypes.

In contrast to the expression of the above-mentioned genes, that of 24 genes was changed in the same direction by *para*^{Shu} and *GstS1*^{M26}. Among these, 17 were up-regulated

and 7 were down-regulated. No GO category was identified for any of the gene sets with P_{adj}<0.05. Interestingly, *GstS1* itself is one of the genes whose expression is down-regulated by both *para*^{Shu} and *GstS1*^{M26}. The observed reduction in levels of *GstS1* expression in the *GstS1*^{M26} mutant is consistent with it being a deletion allele. However, its down-regulation in *para*^{Shu} mutants was unexpected. One possible explanation for this finding is that homeostatic regulation at the level of gene expression counteracts the defects caused by hyperexcitability. It will be important to elucidate the mechanisms by which a gain-of-function mutation in a Na_V-channel gene leads to down-regulation of the expression of its modifier gene and to reduction of the severity of the phenotype.

A previous genetic screen that was similar to ours revealed that loss of the function of *gilgamesh (gish)* reduces the severity of the seizure phenotypes of *para*^{bss} mutant. *gish* encodes the *Drosophila* ortholog of casein kinase CK1γ3, a member of the CK1 family of serine-threonine kinases (HOWLETT *et al.* 2013). Another modifier of seizure activity was discovered by Lin et al. (2017); this group identified *pumilio* (*pum*) based on transcriptome analyses of *Drosophila* seizure models, with *pum* significantly down-regulated in both the genetic (*para*^{bss}) and pharmacological (picrotoxin-induced) models. It was shown that pan-neuronal overexpression of *pum* is sufficient to dramatically reduce seizure severity in *para*^{bss} as well as other seizure-prone *Drosophila* mutants, *easily shocked* (*eas*) and *slamdance* (*sda*) (LIN *et al.* 2017). *pum* encodes RNA binding proteins that act as homeostatic regulators of action potential firing, partly by regulating the translation of *para* transcripts (LIN *et al.* 2017). In addition, we recently discovered that the seizure phenotypes of *para*^{Shu} and other seizure-prone fly mutants are significantly suppressed when the flies are fed a diet supplemented with milk whey (KASUYA *et al.* 2019). It remains unclear how these genetic and environmental factors interact with one another in complex regulatory networks and how they modify the

511 neurological phenotypes of mutants. A mechanistic understanding of such functional
512 interactions is expected to reveal the molecular and cellular processes that are critical for the
513 manifestation of hyperexcitable phenotypes in *Drosophila* mutants, and to provide useful
514 insights into the corresponding processes in vertebrate animals, including humans.

515

516 **FIGURE LEGENDS**

517 **Figure 1. Overlapping deficiencies in the 53E-53F chromosomal region and suppression**
518 **of the climbing defect of *para*^{Shu} mutants.**

519 (A) Chromosomal deficiencies in 53E-53F (right arm of second chromosome) that were
520 examined for effects on *para*^{Shu} phenotypes. The cytological location and chromosomal break
521 points of each deficiency are indicated in the table. (B) Reactive climbing behaviors of *para*^{Shu}
522 heterozygous females in the presence of the tested deficiencies. Three to eight groups of ~20
523 flies per genotype were tested. The total numbers of flies tested in each group were 141
524 (control), 101 (*Df(2R)P803-Δ15*), 93 (*Df(2R)Exel6065*), 111 (*Df(2R)BSC433*), and 53
525 (*Df(2R)Exel6066*). Climbing indices are presented as box plots. The Kruskal-Wallis one-way
526 ANOVA on ranks with Dunn's method was used to compare between the control and
527 deficiency groups. ***P<0.001; NS, not significant (P>0.05).

528 **Figure 2. Suppression of multiple *para*^{Shu} phenotypes by deletion of the genomic region**
529 **53F4-53F8.**

530 The effects of chromosomal deficiencies *Df(2R)BSC273* (49F4-50A13), *Df(2R)BSC330*
531 (51D3-51F9), and *Df(2R)BSC433* (53F4-53F8) on *para*^{Shu} phenotypes were examined. (A)

Frequency of morphological defects, including down-turned wings and an indented thorax. Numbers in the bar graph indicate how many flies were scored. (B) Severity of spontaneous tremors. Numbers in the boxplot indicate how many flies were scored. (C) Severity of heat-induced seizures. Three groups of 30 flies were used per genotype. Data are shown as the averages and SEM. Fisher's exact test with Bonferroni correction (A), the Kruskal-Wallis one-way ANOVA on ranks with Dunn's method (B), and two-way repeated measures ANOVA and Holm-Sidak multiple comparisons (C) were used for comparisons between the control and deficiency groups. ***P<0.001; *P<0.05; NS, not significant (P>0.05).

Figure 3. *Glutathione S-transferase S1* (*GstS1*) as a robust genetic modifier of *para*^{Shu}.

(A) Depiction of six genes that are localized within chromosomal region 53F4-53F8 and disrupted by the chromosomal deficiency *Df(2R)BSC433*. Arrows indicate the direction of gene transcription. (B) The frequency of *para*^{Shu} morphological phenotypes following RNAi-mediated knockdown of each gene. Gene-specific RNAi was ubiquitously expressed using *da-GAl4* in *para*^{Shu} heterozygous females (e.g., *para*^{Shu}/+ ; *da-GAl4*/*UAS*-RNAi). The downturned wing (Wing) and indented thorax (Thorax) phenotypes were scored. Numbers in the bar graph indicate how many flies were scored. Fisher's exact test with Bonferroni correction was used to analyze the data. ***P<0.001; NS, not significant (P>0.05).

Figure 4. *GstS1*^{M26} as a dominant suppressor of *para*^{Shu} phenotypes.

The effects of the *GstS1* null allele, *GstS1*^{M26}, on *para*^{Shu} phenotypes were examined in flies of three genotypes: (1) *para*^{Shu}/+ ; +/+, (2) *para*^{Shu}/+ ; *GstS1*^{M26}/+, and (3) *para*^{Shu}/+ ; *GstS1*^{M26}/*GstS1*^{M26}. (A) Frequencies of down-turned wings (Wings) and indented thorax (Thorax). Numbers in the bar graph indicate how many flies were scored. (B) Severity of

554 spontaneous tremors. 8–10-day-old *para*$^{Shu/+}$ females were used. Numbers in the boxplot
555 indicate how many flies were scored. (C) Frequencies of heat-induced seizures. Three groups
556 of 30-50 flies at 4-5 days after eclosion were used per genotype. Averages are shown with
557 SEM. Fisher's exact test with Bonferroni correction (A), the Kruskal-Wallis one-way ANOVA on
558 ranks with Dunn's method, (B) and two-way repeated measures ANOVA and Holm-Sidak
559 multiple comparisons (C) were used to analyze the data. ***P<0.001; *P<0.05; NS, not
560 significant (P>0.05).

561 **Figure 5. Phenotypes of other neurological mutants are suppressed by *GstS1*^{M26}.**

562 (A) Frequencies of heat-induced seizure at 40ºC in *para*$^{GEFS+}$ plus *GstS1*^{M26} males
563 (*para*$^{GEFS+}$/Y ; *GstS1*^{M26}/+) or *para*$^{GEFS+}$ males (*para*$^{GEFS+}$/Y ; +/+). (B) Frequencies of *para*^{DS}
564 males that did not stand at 37ºC. For (A) and (B), averages of 3 experiments and SEM are
565 shown. In each experiment, 30 flies were examined. (C) Recovery time required for *para*^{bss1}
566 plus *GstS1*^{M26} males (*para*^{bss1}/Y ; *GstS1*^{M26}/+) and *para*^{bss1} males (*para*^{bss1}/Y ; +/+) to recover
567 from paralysis induced by mechanical shock. Data are presented as box plots. Total numbers
568 of flies observed were 127 and 223 flies for *para*^{bss1}/Y ; +/+ and *para*^{bss1}/Y ; *GstS1*^{M26}/+,
569 respectively. Data analysis involved two-way repeated measures ANOVA and Holm-Sidak
570 multiple comparisons (A and B) and the Mann-Whitney *U* test (C). ***P<0.001; *P<0.05; NS,
571 not significant (P>0.05).

572 **Figure 6. Reduction of *GstS1* expression in *para*^{Shu}.**

573 Levels of *GstS1* transcript, as evaluated by RNAseq analysis in control (*Canton-S*) and
574 *para*^{Shu} heterozygous females with or without a *GstS1*^{M26} mutation (*para*^{Shu}/+ ; +/+ or

575 *para*^{Shu}/+ ; *GstS1*^{M26}/+) (see Materials and Methods). Averages of four biological replicates are

576 shown, as normalized read counts with SEM and adjusted *P*-values (P_{adj}). ***P_{adj}<0.001.

REFERENCES

Agianian, B., P. A. Tucker, A. Schouten, K. Leonard, B. Bullard *et al.*, 2003 Structure of a Drosophila sigma class glutathione S-transferase reveals a novel active site topography suited for lipid peroxidation products. J Mol Biol 326**:** 151-165.

Allocati, N., M. Masulli, C. Di Ilio and L. Federici, 2018 Glutathione transferases: substrates, inihibitors and pro-drugs in cancer and neurodegenerative diseases. Oncogenesis 7**:** 8.

Bansal, V., 2017 A computational method for estimating the PCR duplication rate in DNA and RNA-seq experiments. BMC Bioinformatics 18**:** 43.

Benzer, S., 1967 Behavioral mutants of Drosophila isolated by countercurrent distribution. Proc Natl Acad Sci U S A 58**:** 1112-1119.

Besson, M., and J. R. Martin, 2005 Centrophobism/thigmotaxis, a new role for the mushroom bodies in Drosophila. J Neurobiol 62**:** 386-396.

Catterall, W. A., 2012 Voltage-gated sodium channels at 60: structure, function and pathophysiology. J Physiol 590**:** 2577-2589.

Catterall, W. A., F. Kalume and J. C. Oakley, 2010 NaV1.1 channels and epilepsy. J Physiol 588**:** 1849-1859.

Chung, H., T. Sztal, S. Pasricha, M. Sridhar, P. Batterham *et al.*, 2009 Characterization of Drosophila melanogaster cytochrome P450 genes. Proc Natl Acad Sci U S A 106**:** 5731-5736.

596 Claes, L., J. Del-Favero, B. Ceulemans, L. Lagae, C. Van Broeckhoven *et al.*, 2001 De novo
597 mutations in the sodium-channel gene SCN1A cause severe myoclonic epilepsy of
598 infancy. Am J Hum Genet 68**:** 1327-1332.

599 Cook, R. K., S. J. Christensen, J. A. Deal, R. A. Coburn, M. E. Deal *et al.*, 2012 The generation
600 of chromosomal deletions to provide extensive coverage and subdivision of the
601 Drosophila melanogaster genome. Genome Biol 13**:** R21.

602 Csala, M., T. Kardon, B. Legeza, B. Lizak, J. Mandl *et al.*, 2015 On the role of 4-
603 hydroxynonenal in health and disease. Biochim Biophys Acta 1852**:** 826-838.

604 Davis, R. C., A. Diep, W. Hunziker, I. Klisak, T. Mohandas *et al.*, 1991 Assignment of human
605 pancreatic lipase gene (PNLIP) to chromosome 10q24-q26. Genomics 11**:** 1164-1166.

606 Dib-Hajj, S. D., J. A. Black and S. G. Waxman, 2015 NaV1.9: a sodium channel linked to
607 human pain. Nature Reviews Neuroscience 16**:** 511.

608 Ganetzky, B., and C. F. Wu, 1982 Indirect Suppression Involving Behavioral Mutants with
609 Altered Nerve Excitability in DROSOPHILA MELANOGASTER. Genetics 100**:** 597-614.

610 Gilestro, G. F., and C. Cirelli, 2009 pySolo: a complete suite for sleep analysis in Drosophila.
611 Bioinformatics 25**:** 1466-1467.

612 Hales, K. G., C. A. Korey, A. M. Larracuente and D. M. Roberts, 2015 Genetics on the Fly: A
613 Primer on the Drosophila Model System. Genetics 201**:** 815-842.

614 Hannemann, F., A. Bichet, K. M. Ewen and R. Bernhardt, 2007 Cytochrome P450 systems--
615 biological variations of electron transport chains. Biochim Biophys Acta 1770**:** 330-344.

Hayes, J. D., J. U. Flanagan and I. R. Jowsey, 2005 Glutathione transferases. Annu Rev Pharmacol Toxicol 45**:** 51-88.

Hodgkin, A. L., and A. F. Huxley, 1952 A quantitative description of membrane current and its application to conduction and excitation in nerve. J Physiol 117**:** 500-544.

Howlett, I. C., Z. M. Rusan, L. Parker and M. A. Tanouye, 2013 Drosophila as a model for intractable epilepsy: gilgamesh suppresses seizures in para(bss1) heterozygote flies. G3 (Bethesda) 3**:** 1399-1407.

Hu, Y., I. Flockhart, A. Vinayagam, C. Bergwitz, B. Berger *et al.*, 2011 An integrative approach to ortholog prediction for disease-focused and other functional studies. BMC Bioinformatics 12**:** 357.

Imai, Y., M. Soda and R. Takahashi, 2000 Parkin suppresses unfolded protein stress-induced cell death through its E3 ubiquitin-protein ligase activity. J Biol Chem 275**:** 35661-35664.

Isin, E. M., and F. P. Guengerich, 2007 Complex reactions catalyzed by cytochrome P450 enzymes. Biochim Biophys Acta 1770**:** 314-329.

Jen, J. C., T. Ashizawa, R. C. Griggs and M. F. Waters, 2016 Rare neurological channelopathies — networks to study patients, pathogenesis and treatment. Nature Reviews Neurology 12**:** 195.

Joo, M., and R. T. Sadikot, 2012 PGD synthase and PGD2 in immune resposne. Mediators Inflamm 2012**:** 503128.

636 Kaas, G. A., J. Kasuya, P. Lansdon, A. Ueda, A. Iyengar *et al.*, 2016 Lithium-Responsive
637 Seizure-Like Hyperexcitability Is Caused by a Mutation in the Drosophila Voltage-Gated
638 Sodium Channel Gene paralytic. eNeuro 3.

639 Kasuya, J., A. Iyengar, H. L. Chen, P. Lansdon, C. F. Wu *et al.*, 2019 Milk-whey diet
640 substantially suppresses seizure-like phenotypes of para(Shu), a Drosophila voltage-
641 gated sodium channel mutant. J Neurogenet**:** 1-15.

642 Klassen, T., C. Davis, A. Goldman, D. Burgess, T. Chen *et al.*, 2011 Exome sequencing of ion
643 channel genes reveals complex profiles confounding personal risk assessment in
644 epilepsy. Cell 145**:** 1036-1048.

645 Kroll, J. R., A. Saras and M. A. Tanouye, 2015 Drosophila sodium channel mutations:
646 Contributions to seizure-susceptibility. Exp Neurol.

647 Lilly, M., R. Kreber, B. Ganetzky and J. R. Carlson, 1994 Evidence that the Drosophila
648 olfactory mutant smellblind defines a novel class of sodium channel mutation. Genetics
649 136**:** 1087-1096.

650 Lin, W. H., C. N. Giachello and R. A. Baines, 2017 Seizure control through genetic and
651 pharmacological manipulation of Pumilio in Drosophila: a key component of neuronal
652 homeostasis. Dis Model Mech 10**:** 141-150.

653 Lindsay, H. A., R. Baines, R. ffrench-Constant, K. Lilley, H. T. Jacobs *et al.*, 2008 The
654 dominant cold-sensitive Out-cold mutants of Drosophila melanogaster have novel
655 missense mutations in the voltage-gated sodium channel gene paralytic. Genetics 180**:**
656 873-884.

657 Love, M. I., W. Huber and S. Anders, 2014 Moderated estimation of fold change and
658 dispersion for RNA-seq data with DESeq2. Genome Biol 15**:** 550.

659 Martin, R. L., B. Pittendrigh, J. Liu, R. Reenan, R. ffrench-Constant *et al.*, 2000 Point mutations
660 in domain III of a Drosophila neuronal Na channel confer resistance to allethrin. Insect
661 Biochem Mol Biol 30**:** 1051-1059.

662 Parker, L., M. Padilla, Y. Du, K. Dong and M. A. Tanouye, 2011 Drosophila as a model for
663 epilepsy: bss is a gain-of-function mutation in the para sodium channel gene that leads
664 to seizures. Genetics 187**:** 523-534.

665 Rajakariar, R., M. Hilliard, T. Lawrence, S. Trivedi, P. Colville-Nash *et al.*, 2007 Hematopoietic
666 prostaglandin D2 synthase controls the onset and resolution of acute inflammation
667 through PGD2 and 15-deoxyDelta12 14 PGJ2. Proc Natl Acad Sci U S A 104**:** 20979-
668 20984.

669 Rajakulendran, S., D. Kaski and M. G. Hanna, 2012 Neuronal P/Q-type calcium channel
670 dysfunction in inherited disorders of the CNS. Nature Reviews Neurology 8**:** 86-96.

671 Regan, J. C., A. S. Brandao, A. B. Leitao, A. R. Mantas Dias, E. Sucena *et al.*, 2013 Steroid
672 hormone signaling is essential to regulate innate immune cells and fight bacterial
673 infection in Drosophila. PLoS Pathog 9**:** e1003720.

674 Roote, J., and S. Russell, 2012 Toward a complete Drosophila deficiency kit. Genome Biol 13**:**
675 149.

676 Saisawang, C., J. Wongsantichon and A. J. Ketterman, 2012 A preliminary characterization of
677 the cytosolic glutathione transferase proteome from Drosophila melanogaster. Biochem
678 J 442**:** 181-190.

679 Sajjadian, S. M., S. Ahmed, M. A. Al Baki and Y. Kim, 2019 Prostaglandin D2 synthase and its
680 functional association with immune and reproductive processes in a lepidopteran insect,
681 Spodoptera exigua. Gen Comp Endocrinol 287**:** 113352.

682 Scarpati, M., Y. Qi, S. Govind and S. Singh, 2019 A combined computational strategy of
683 sequence and structural analysis predicts the existence of a functional eicosanoid
684 pathway in Drosophila melanogaster. PLoS One 14**:** e0211897.

685 Schutte, R. J., S. S. Schutte, J. Algara, E. V. Barragan, J. Gilligan *et al.*, 2014 Knock-in model
686 of Dravet syndrome reveals a constitutive and conditional reduction in sodium current. J
687 Neurophysiol 112**:** 903-912.

688 Shimura, H., N. Hattori, S. Kubo, Y. Mizuno, S. Asakawa *et al.*, 2000 Familial Parkinson
689 disease gene product, parkin, is a ubiquitin-protein ligase. Nat Genet 25**:** 302-305.

690 Shoeb, M., N. H. Ansari, S. K. Srivastava and K. V. Ramana, 2014 4-Hydroxynonenal in the
691 pathogenesis and progression of human diseases. Curr Med Chem 21**:** 230-237.

692 Singh, S. P., J. A. Coronella, H. Benes, B. J. Cochrane and P. Zimniak, 2001 Catalytic function
693 of Drosophila melanogaster glutathione S-transferase DmGSTS1-1 (GST-2) in
694 conjugation of lipid peroxidation end products. Eur J Biochem 268**:** 2912-2923.

695 Stofanko, M., S. Y. Kwon and P. Badenhorst, 2008 A misexpression screen to identify
696 regulators of Drosophila larval hemocyte development. Genetics 180**:** 253-267.

Sun, L., J. Gilligan, C. Staber, R. J. Schutte, V. Nguyen *et al.*, 2012 A knock-in model of human epilepsy in Drosophila reveals a novel cellular mechanism associated with heat-induced seizure. J Neurosci 32**:** 14145-14155.

Suzuki, D. T., T. Grigliatti and R. Williamson, 1971 Temperature-sensitive mutations in Drosophila melanogaster. VII. A mutation (para-ts) causing reversible adult paralysis. Proc Natl Acad Sci U S A 68**:** 890-893.

Theken, K. N., Y. Deng, M. A. Kannon, T. M. Miller, S. M. Poloyac *et al.*, 2011 Activation of the acute inflammatory response alters cytochrome P450 expression and eicosanoid metabolism. Drug Metab Dispos 39**:** 22-29.

Tu, C. P., and B. Akgul, 2005 Drosophila glutathione S-transferases. Methods Enzymol 401**:** 204-226.

Ugur, B., K. Chen and H. J. Bellen, 2016 Drosophila tools and assays for the study of human diseases. Dis Model Mech 9**:** 235-244.

Venetucci, L., M. Denegri, C. Napolitano and S. G. Priori, 2012 Inherited calcium channelopathies in the pathophysiology of arrhythmias. Nature Reviews Cardiology 9**:** 561-575.

Waxman, S. G., and G. W. Zamponi, 2014 Regulating excitability of peripheral afferents: emerging ion channel targets. Nature Neuroscience 17**:** 153.

Whitworth, A. J., D. A. Theodore, J. C. Greene, H. Benes, P. D. Wes *et al.*, 2005 Increased glutathione S-transferase activity rescues dopaminergic neuron loss in a Drosophila model of Parkinson's disease. Proc Natl Acad Sci U S A 102**:** 8024-8029.

718 Williamson, R. L., 1982 Lithium stops hereditary shuddering in Drosophila melanogaster.
719 Psychopharmacology (Berl) 76**:** 265-268.

720 Williamson, R. L. M., 1971 The isolation and study of two mutants affecting motor activity in
721 Drosophila melanogaster, pp. in *Zoology*. University British Columbia, Vancouver.

722 Young, M. D., M. J. Wakefield, G. K. Smyth and A. Oshlack, 2010 Gene ontology analysis for
723 RNA-seq: accounting for selection bias. Genome Biol 11**:** R14.

724 Zhang, H., and H. J. Forman, 2017 4-hydroxynonenal-mediated signaling and aging. Free
725 Radic Biol Med 111**:** 219-225.

726 Zhang, H., J. Tan, E. Reynolds, D. Kuebler, S. Faulhaber *et al.*, 2002 The Drosophila
727 slamdance gene: a mutation in an aminopeptidase can cause seizure, paralysis and
728 neuronal failure. Genetics 162**:** 1283-1299.

729 Zhang, Y., J. Gao, K. K. Chung, H. Huang, V. L. Dawson *et al.*, 2000 Parkin functions as an
730 E2-dependent ubiquitin- protein ligase and promotes the degradation of the synaptic
731 vesicle-associated protein, CDCrel-1. Proc Natl Acad Sci U S A 97**:** 13354-13359.

732

Table 1. Effects of *GstS1^{M26}* on viability and fertility of *para^{Shu}* males

Genotype	Viability				Fertility			
	Total	*FM7*/Y	*para^{Shu}*/Y	% *para^{Shu}*/Y	Total	Sterile	Fertile	% Fertile
para^{Shu}/Y ; +/+	73	67	6	8.2	43	42	1	2.3
para^{Shu}/Y ; *GstS1^{M26}*/+	121	83	38	31.4	45	28	17	37.8
para^{Shu}/Y ; *GstS1^{M26}*/*GstS1^{M26}*	145	68	77	53.1	44	27	17	38.6

Table 2. Effects of GST gene deletions on wing and thorax phenotypes of *para*^{Shu}/+

Chromosomal deficiency	Deleted segment	Deleted GST genes	Flies scored	Down-turned wings		Indented thorax	
				(%)	(*P*-value)	(%)	(*P*-value)
Df(3R)Exel6164	87B5-87B10	*GstD1-D11*	72	95.8	0.154	62.5	0.001*
Df(2R)BSC335	55C6-55F1	*GstE1-E11*	59	91.5	0.741	86.4	0.550
Df(2R)BSC856	60E1-60E4	*GstE12*	68	77.9	0.208	83.8	0.397
Df(2R)BSC271	44F12-45A12	*GstE13*	67	94.0	0.480	77.6	0.0775
Df(2R)BSC273	49F4-50A13	*GstE14*	66	92.4	0.517	90.9	1
Df(3L)BSC157	66C12-66D6	*GstO1-O4*	150	94.7	0.175	70.0	0.0052
Df(2R)BSC132	45F6-46B4	*GstT1-T2*	51	68.6	0.025	9.80	<0.00001*
Df(1)Exel6254	19C4-19D1	*GstT3*	34	91.2	1	94.2	0.691
Df(1)Exel6245	11E11-11F4	*GstT4*	26	23.1	<0.00001*	80.8	0.277
Df(3R)by10	85D8-85E13	*GstZ1-Z2*	57	89.5	1	91.2	1
Df(2R)BSC433	53F4-53F8	*GstS1*	56	12.5	<0.00001*	35.7	<0.00001*
No deficiency	NA	NA	44	88.6	NA	90.9	NA

Statistical significance in the severity of wing and thorax phenotypes between *para*^{Shu} (*para*^{Shu}/+) and *para*^{Shu} with a deficiency (*para*^{Shu}/+ ; *Df*/+ or *para*^{Shu}/*Df*) was assessed using Fisher's exact test. The *P*-values were compared to Bonferroni adjusted type I error rate of 0.05/11 (=0.004545·····) for significance (*). NA, not applicable.

Table 3A. Enriched GO terms that are overrepresented in differentially expressed genes in *para*^{Shu}/+ compared with control

Gene ontology	Term	Ontology class	P_{adj} over-represented value	# of genes
GO:0008010	structural constituent of chitin-based larval cuticle	MF	8.83E-3	8
GO:0005214	structural constituent of chitin-based cuticle	MF	1.05E-2	8
GO:0042302	structural constituent of cuticle	MF	1.24E-2	8
GO:0040003	chitin-based cuticle development	BP	2.01E-2	9

MF: molecular function, BP: biological process.

Table 3B. Differentially expressed genes in *para*^{Shu} /+ compared with control that are included in the enriched GO terms

Flybase ID	Gene symbol	Fold change (log2)	Fold change	P_{adj}	Gene product
FBgn0033603	*Cpr47Ef*	1.14	2.20	2.03E-11	Cuticular protein 47Ef
FBgn0004782	*Ccp84Ab*	1.02	2.03	1.83E-10	Ccp84Ab
FBgn0004783	*Ccp84Aa*	0.92	1.89	9.93E-05	Ccp84Aa
FBgn0001112	*Gld*	0.73	1.66	3.22E-03	Glucose dehydrogenase
FBgn0004780	*Ccp84Ad*	0.72	1.65	1.02E-02	Ccp84Ad
FBgn0035281	*Cpr62Bc*	0.64	1.56	3.59E-03	Cuticular protein 62Bc
FBgn0036619	*Cpr72Ec*	0.64	1.55	3.97E-02	Cuticular protein 72Ec
FBgn0036680	*Cpr73D*	0.514	1.43	3.35E-02	Cuticular protein 73D
FBgn0052029	*Cpr66D*	-0.68	0.62	9.58E-03	Cuticular protein 66D

Table 4. Genes most differentially expressed in *para*^{Shu}/+ compared with control

Flybase ID	Gene symbol	Fold change (log2)	Fold change	P_{adj}	Gene product
FBgn0052581	*CG32581*	3.78	13.75	5.26E-99	uncharacterized protein
FBgn0010549	*l(2)03659*	2.44	5.43	3.70E-40	lethal (2) 03659
FBgn0020906	*Jon25Bi*	1.72	3.29	4.84E-18	Jonah 25Bi
FBgn0052523	*CG32523*	1.66	3.17	3.83E-19	uncharacterized protein
FBgn0004427	*LysD*	1.47	2.77	2.68E-13	Lysozyme D
FBgn0004426	*LysC*	1.46	2.76	7.84E-14	Lysozyme C
FBgn0015037	*Cyp4p1*	1.35	2.55	6.95E-15	Cytochrome P450-4p1
FBgn0033065	*Cyp6w1*	1.30	2.47	3.77E-15	Cyp6w1
FBgn0032286	*CG7300*	1.20	2.30	2.47E-08	uncharacterized protein
FBgn0031169	*CG1494*	1.20	2.30	4.50E-08	uncharacterized protein
FBgn0033603	*Cpr47Ef*	1.14	2.20	2.03E-11	Cuticular protein 47Ef
FBgn0039039	*lmd*	1.11	2.16	5.21E-07	lame duck
FBgn0033458	*CG18446*	1.10	2.14	7.42E-08	uncharacterized protein
FBgn0051865	*Ada1-1*	1.09	2.12	7.74E-08	transcriptional Adaptor 1-1
FBgn0036833	*CG3819*	1.07	2.11	1.12E-17	uncharacterized protein
FBgn0004782	*Ccp84Ab*	1.02	2.03	1.83E-10	Ccp84Ab

Listed are genes differentially expressed in *para*^{Shu} compared with control (*Canton-S*) with Fold change > 2 and $P_{adj} < 0.01$.

Table 5. Expression levels of GST genes in control and *para*^{Shu}/+

GST genes	Flybase ID	average of normalized counts (DESeq2)		Fold change (log2)	Fold change	P_{adj}
		Control	*para*^{Shu}			
GstS1	FBgn0063499	15562.21	7782.01	-0.76	0.59	<0.001***
GstD1	FBgn0063495	10428.37	10078.77	-0.02	0.99	1.000
GstD2	FBgn0010041	175.19	54.34	-0.72	0.61	0.010*
GstD3	FBgn0037696	315.48	208.52	-0.20	0.87	1.000
GstD4	FBgn0063492	6.43	5.55	-0.06	0.96	1.000
GstD5	FBgn0063498	43.77	20.34	-0.32	0.80	0.878
GstD6	FBgn0010043	2.45	4.40	0.14	1.10	1.000
GstD7	FBgn0050000	75.87	83.37	0.07	1.05	1.000
GstD8	FBgn0086348	50.70	55.24	0.06	1.04	1.000
GstD9	FBgn0010044	373.48	431.20	0.10	1.07	1.000
GstD10	FBgn0063497	126.21	176.08	0.30	1.23	1.000
GstD11	FBgn0037697	34.52	43.76	0.18	1.13	1.000
GstE1	FBgn0033381	934.78	894.99	-0.05	0.97	1.000
GstE2	FBgn0010226	63.43	77.50	0.18	1.13	1.000
GstE3	FBgn0010042	679.13	697.94	0.02	1.01	1.000
GstE4	FBgn0033817	89.15	101.79	0.14	1.10	1.000
GstE5	FBgn0063491	203.55	227.27	0.10	1.07	1.000
GstE6	FBgn0038029	2026.31	1985.35	-0.02	0.99	1.000
GstE7	FBgn0001149	561.78	493.62	-0.09	0.94	1.000
GstE8	FBgn0035906	410.02	375.98	-0.06	0.96	1.000
GstE9	FBgn0010039	887.16	1218.13	0.39	1.31	0.206
GstE10	FBgn0063493	90.21	111.71	0.17	1.13	1.000
GstE11	FBgn0042206	287.81	283.10	-0.02	0.99	1.000
GstE12	FBgn0030484	4456.11	4955.73	0.11	1.08	1.000
GstE13	FBgn0038020	922.06	894.20	-0.02	0.99	1.000
GstE14	FBgn0035904	118.30	136.79	0.12	1.09	1.000
GstO1	FBgn0035907	604.75	547.12	-0.09	0.94	1.000

GstO2	FBgn0063494	1408.05	2117.33	0.52	1.43	0.002**
GstO3	FBgn0034354	816.42	835.42	0.03	1.02	1.000
GstO4	FBgn0050005	171.63	192.39	0.13	1.09	1.000
GstT1	FBgn0031117	1085.64	998.88	-0.07	0.95	1.000
GstT2	FBgn0034335	511.60	386.89	-0.32	0.80	0.705
GstT3	FBgn0063496	639.30	587.15	-0.11	0.93	1.000
GstT4	FBgn0010040	2218.35	2405.08	0.10	1.07	1.000
GstZ1	FBgn0027590	306.76	252.35	-0.24	0.85	1.000
GstZ2	FBgn0010038	272.48	246.37	-0.09	0.94	1.000

Transcript levels of the 36 genes encoding soluble GSTs were evaluated by DEseq2 analysis of four biological replicates in control (*Canton-S*) and $para^{Shu}$. Adjusted P-values (P_{adj}) were obtained using Benjamini-Hochberg (BH) procedure (*P_{adj} <0.05; **P_{adj} <0.01; ***P_{adj} <0.001).

Table 6A. Enriched GO terms that are overrepresented in differentially expressed genes in *para^{Shu}/+; GstS1^{M26}/+ compared with para^{Shu}/+; +/+*

Gene ontology	Term	Ontology class	P_{adj} over-represented value	# of genes
GO:0020037	heme binding	MF	7.31E-4	14
GO:0046906	tetrapyrrole binding	MF	7.31E-4	14
GO:0005506	iron ion binding	MF	1.53E-3	14
GO:0016705	oxidoreductase activity, acting on paired donors, with incorporation or reduction of molecular oxygen	MF	2.83E-3	14
GO:0048037	cofactor binding	MF	4.60E-3	21

MF: molecular function

Table 6B. Differentially expressed genes in *para^{Shu}/+; GstS1^{M26}/+ compared with para^{Shu}/+; +/+* that are included in the enriched GO terms

Flybase ID	Gene symbol	Fold change (log2)	Fold change	P_{adj}	Gene product
FBgn0013772	*Cyp6a8**	1.69	3.22	9.37E-20	Cytochrome P450-6a8
FBgn0000473	*Cyp6a2**	1.51	2.84	6.10E-15	Cytochrome P450-6a2
FBgn0041337	*Cyp309a2**	1.11	2.16	1.07E-07	Cyp309a2
FBgn0033978	*Cyp6a23**	1.05	2.07	7.16E-15	Cyp6a23
FBgn0033980	*Cyp6a20**	0.80	1.74	4.29E-04	Cyp6a20
FBgn0033983	*ADPS*	0.78	1.72	9.71E-08	Alkyldihydroxyacetone-phosphate synthase
FBgn0015039	*Cyp9b2**	0.68	1.60	5.52E-07	Cytochrome P450-9b2
FBgn0031689	*Cyp28d1**	0.66	1.58	8.28E-06	Cyp28d1
FBgn0015037	*Cyp4p1**	0.59	1.51	2.79E-04	Cytochrome P450-4p1
FBgn0036381	*CG8745*	-0.37	0.78	4.09E-02	uncharacterized protein
FBgn0003965	*v*	-0.38	0.77	4.06E-02	vermilion
FBgn0035906	*GstO2*	-0.41	0.75	1.59E-02	Glutathione S transferase O2

FBgn0036927	*Gabat*	-0.49	0.71	1.13E-04	gamma-aminobutyric acid transaminase
FBgn0000566	*Eip55E*	-0.54	0.69	1.27E-04	Ecdysone-induced protein 55E
FBgn0051674	*CG31674*	-0.55	0.68	8.18E-03	uncharacterized protein
FBgn0029172	*Fad2*	-0.79	0.58	1.60E-05	Fad2
FBgn0015040	*Cyp9c1**	-0.79	0.58	7.31E-06	Cytochrome P450-9c1
FBgn0034756	*Cyp6d2**	-0.80	0.58	5.96E-09	Cyp6d2
FBgn0001112	*Gld*	-0.95	0.52	1.43E-06	Glucose dehydrogenase
FBgn0031925	*Cyp4d21**	-0.95	0.52	8.28E-06	Cyp4d21
FBgn0015714	*Cyp6a17**	-1.04	0.49	2.76E-15	Cytochrome P450-6a17
FBgn0033395	*Cyp4p2**	-2.68	0.16	3.51E-48	Cyp4p2

* indicates genes that belong to GO:0020037, GO:0046906, GO:0005506 and GO:0016705.

Table 7. Genes most differentially expressed in *para^{Shu}*/+ ; *GstS1^{M26}*/+ compared with *para^{Shu}*/+ ; +/+

Flybase ID	Gene symbol	Fold change (log2)	Fold change	P_{adj}	Gene product
FBgn0085732	*CR40190*	2.12	4.36	1.32E-29	pseudo
FBgn0033954	*CG12860*	2.02	4.05	1.42E-26	uncharacterized protein
FBgn0039752	*CG15530*	1.95	3.86	7.79E-30	uncharacterized protein
FBgn0037850	*CG14695*	1.90	3.73	1.32E-29	uncharacterized protein
FBgn0033748	*vis*	1.90	3.72	1.91E-23	vismay
FBgn0266084	*Fhos*	1.85	3.60	6.52E-32	Formin homology 2 domain containing
FBgn0040104	*lectin-24A*	1.76	3.38	5.28E-20	lectin-24A
FBgn0013772	*Cyp6a8*	1.69	3.22	9.38E-20	Cytochrome P450-6a8
FBgn0031935	*CG13793*	1.63	3.09	1.28E-22	uncharacterized protein
FBgn0000473	*Cyp6a2*	1.51	2.84	6.10E-15	Cytochrome P450-6a2
FBgn0033926	*Arc1*	1.42	2.67	4.34E-25	Activity-regulated cytoskeleton associated protein 1
FBgn0085452	*CG34423*	1.37	2.58	1.77E-12	uncharacterized protein
FBgn0259896	*NimC1*	1.35	2.54	1.51E-13	Nimrod C1
FBgn0261055	*Sfp26Ad*	1.28	2.43	8.50E-11	Seminal fluid protein 26Ad
FBgn0003082	*phr*	1.27	2.41	1.06E-23	photorepair
FBgn0003961	*Uro*	1.19	2.28	1.17E-14	Urate oxidase
FBgn0013308	*Odc2*	1.16	2.23	1.61E-08	Ornithine decarboxylase 2
FBgn0004426	*LysC*	1.12	2.18	5.61E-08	Lysozyme C
FBgn0052198	*CG32198*	1.12	2.17	3.25E-08	uncharacterized protein
FBgn0041337	*Cyp309a2*	1.11	2.16	1.07E-07	Cyp309a2
FBgn0053511	*CG33511*	1.10	2.14	1.07E-07	uncharacterized protein
FBgn0034783	*CG9825*	1.09	2.12	1.95E-07	uncharacterized protein

FBgn0032210	*CYLD*	1.05	2.07	7.58E-11	Cylindromatosis
FBgn0033978	*Cyp6a23*	1.05	2.07	7.16E-15	Cyp6a23
FBgn0004425	*LysB*	1.03	2.04	1.13E-06	Lysozyme B
FBgn0004782	*Ccp84Ab*	-1.01	0.50	9.43E-07	Ccp84Ab
FBgn0034715	*Oatp58Db*	-1.01	0.50	1.05E-11	Organic anion transporting polypeptide 58Db
FBgn0037292	*plh*	-1.02	0.49	7.84E-12	pasang lhamu
FBgn0015714	*Cyp6a17*	-1.04	0.49	2.76E-15	Cytochrome P450-6a17
FBgn0030815	*CG8945*	-1.09	0.47	3.08E-08	uncharacterized protein
FBgn0004783	*Ccp84Aa*	-1.10	0.47	1.11E-07	Ccp84Aa
FBgn0250825	*CG34241*	-1.21	0.43	3.92E-10	uncharacterized protein
FBgn0034356	*Pepck2*	-1.29	0.41	8.57E-12	Phosphoenolpyruvate carboxykinase 2
FBgn0031533	*CG2772*	-1.45	0.37	4.15E-29	uncharacterized protein
FBgn0031741	*CG11034*	-1.54	0.35	1.23E-18	uncharacterized protein
FBgn0260874	*Ir76a*	-1.68	0.31	7.94E-19	Ionotropic receptor 76a
FBgn0033395	*CR40190*	-2.68	0.16	3.51E-48	Cyp4p2

Listed are genes differentially expressed in $para^{Shu}$/+ ; $GstS1^{M26}$/+ compared with $para^{Shu}$/+ ; +/+ with Fold change > 2 and $P_{adj} < 0.01$.

Figure 1

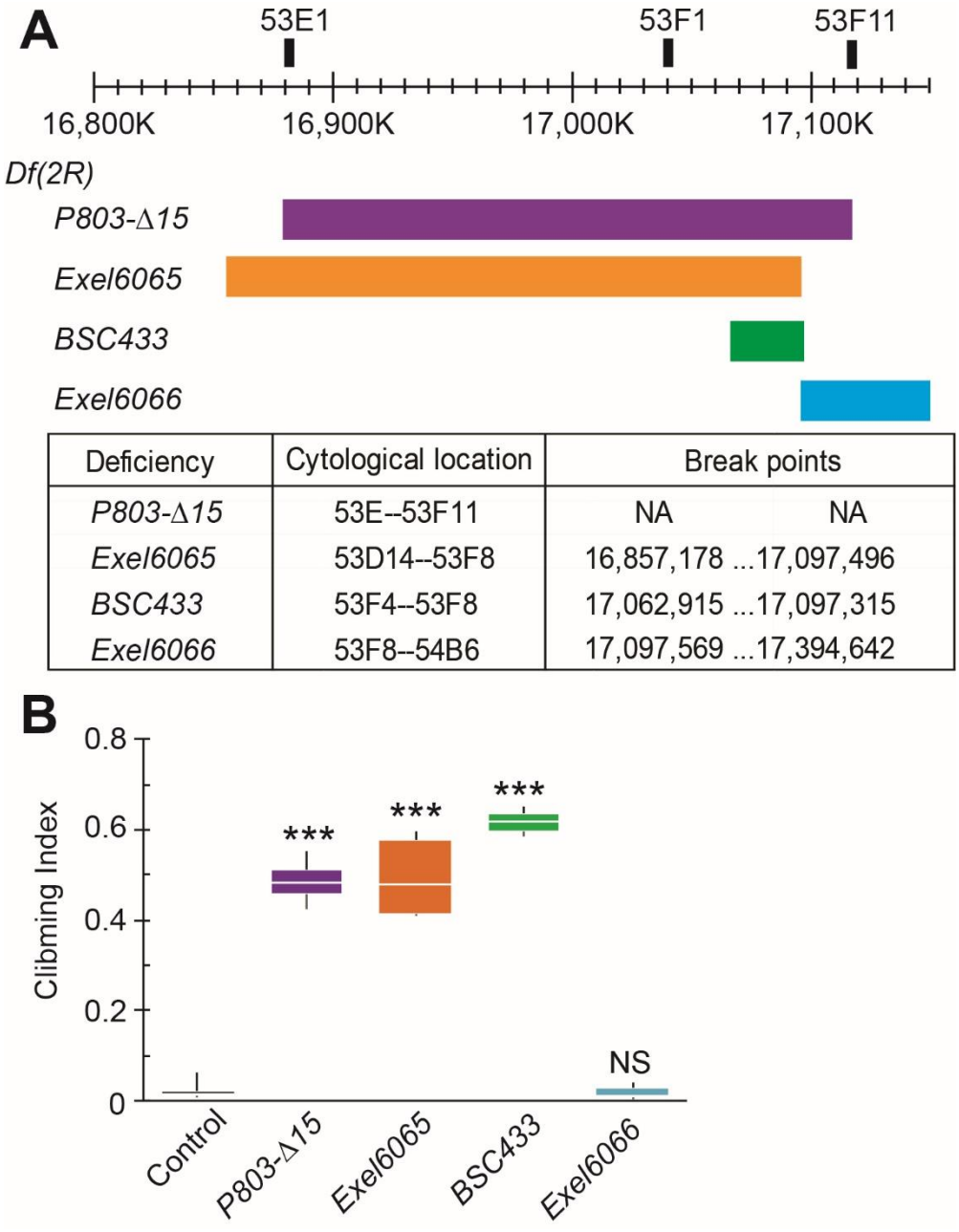

Deficiency	Cytological location	Break points	
P803-Δ15	53E--53F11	NA	NA
Exel6065	53D14--53F8	16,857,178	...17,097,496
BSC433	53F4--53F8	17,062,915	...17,097,315
Exel6066	53F8--54B6	17,097,569	...17,394,642

Figure 2

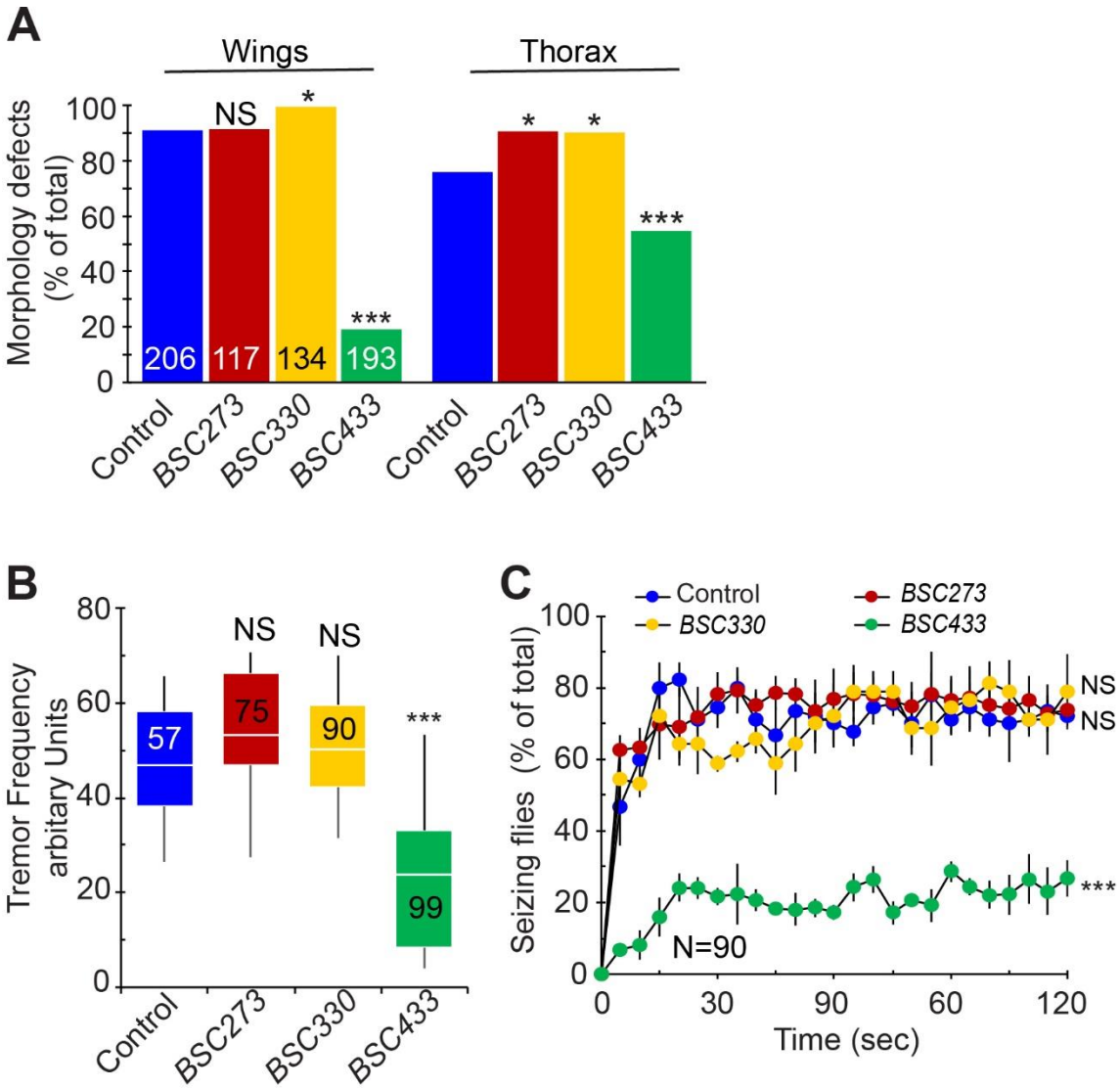

Figure 3

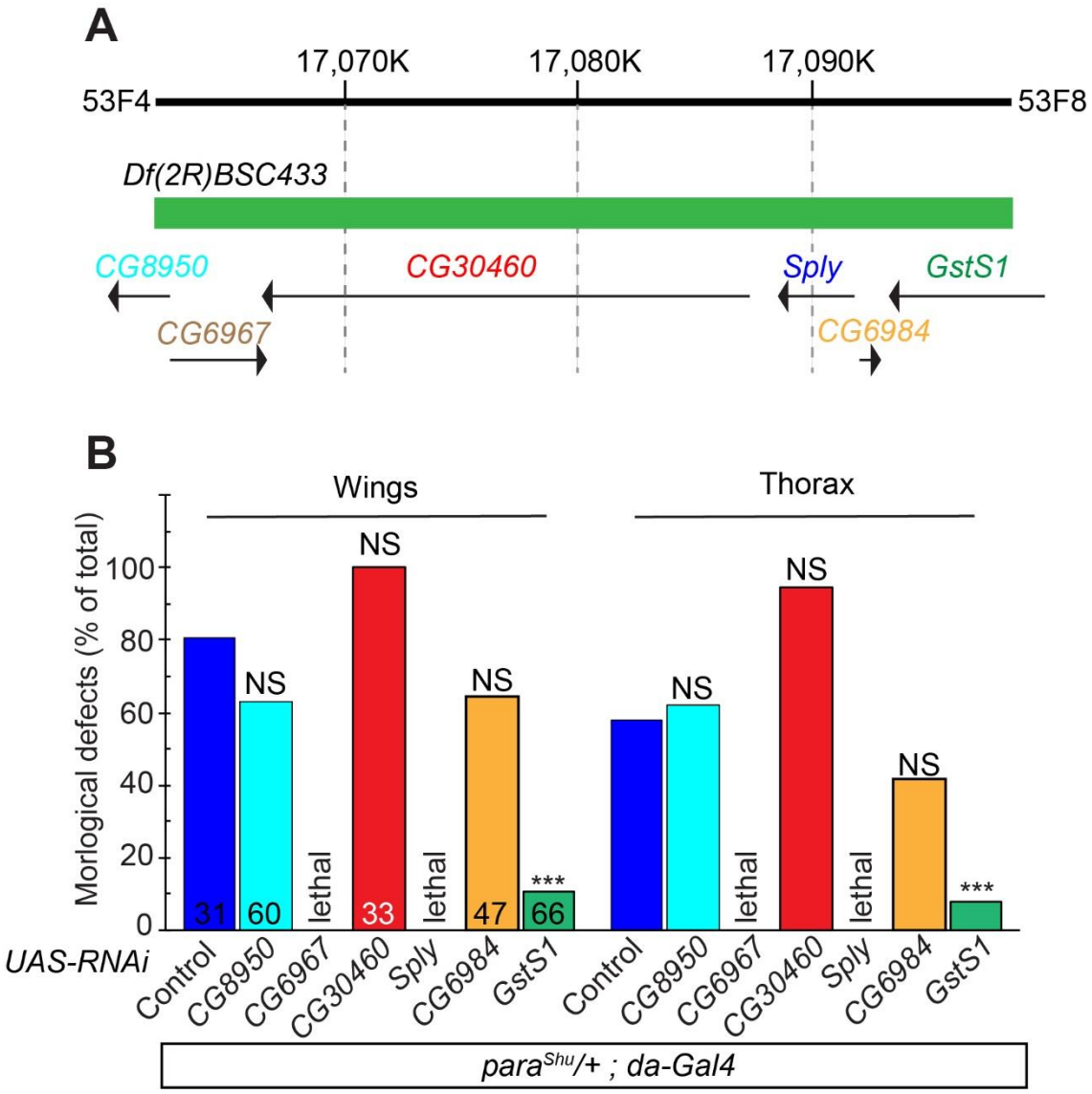

Figure 4

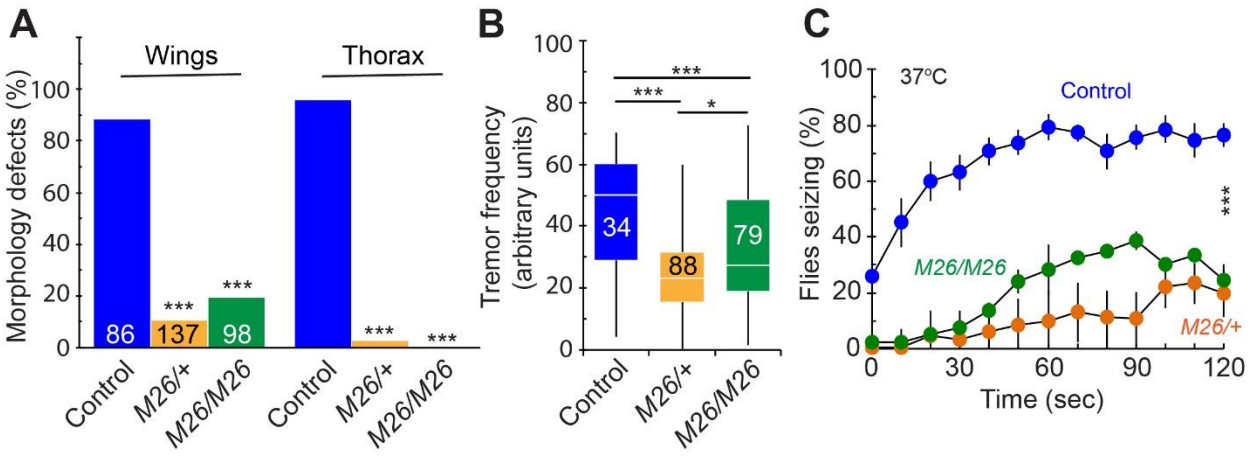

Figure 5

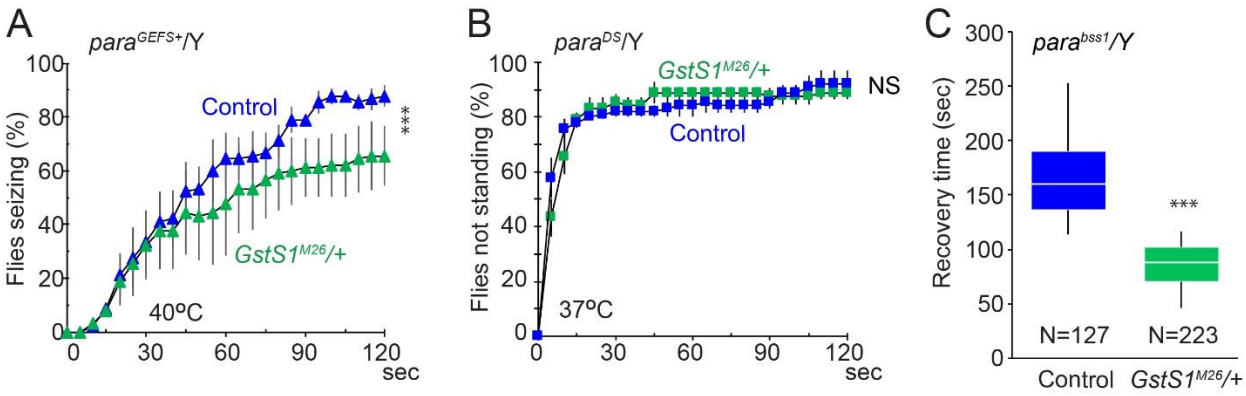

Figure 6